Transit navigation through Northern Sea Route from satellite data and CMIP5 simulations

2017 Environ. Res. Lett. 12 024010

(http://iopscience.iop.org/1748-9326/12/2/024010)

Environmental Research Letters

CrossMark

OPEN ACCESS

RECEIVED
1 October 2016

REVISED
22 December 2016

ACCEPTED FOR PUBLICATION
10 January 2017

PUBLISHED
7 February 2017

LETTER

Transit navigation through Northern Sea Route from satellite data and CMIP5 simulations

Vyacheslav C Khon[1,2,5], Igor I Mokhov[1,3] and Vladimir A Semenov[1,4]

1 A.M. Obukhov Institute of Atmospheric Physics, Russian Academy of Sciences, Moscow, Russia
2 Institute of Geosciences at Kiel University, Kiel, Germany
3 Lomonosov Moscow State University, Moscow, Russia
4 Institute of Geography, Russian Academy of Sciences, Moscow, Russia
5 Author to whom any correspondence should be addressed.

E-mail: khon@ifaran.ru

Keywords: Northern Sea Route, arctic marine navigation, climate models, Arctic sea ice

Supplementary material for this article is available online

Abstract

Rapid Arctic sea ice decline over the last few decades opens new perspectives for Arctic marine navigation. Further warming in the Arctic will promote the Northern Sea Route (NSR) as an alternative to the conventional Suez or Panama Canal routes for intercontinental shipping. Here we use both satellite data and CMIP5 ensemble of climate models to estimate the NSR transit window allowing intercontinental navigation between Atlantic and Pacific regions. To this end, we introduce a novel approach to calculate start and end dates of the navigation season along the NSR. We show that modern climate models are able to reproduce the mean time of the NSR transit window and its trend over the last few decades. The selected models demonstrate that the rate of increase of the NSR navigation season will slow down over the next few decades with the RCP4.5 scenario. By the end of the 21st century ensemble-mean estimates show an increase of the NSR transit window by about 4 and 6.5 months according to RCP4.5 and 8.5, respectively. Estimated trends for the end date of the navigation season are found to be stronger compared to those for the start date.

1. Introduction

Rapid Arctic sea ice retreat during the last few decades has had major impacts on Arctic marine transport systems and shelf exploration. Climate models project further decrease of sea ice cover in the 21st century accompanied by changes in variability and amplitude of seasonal cycle (e.g. Stroeve *et al* 2012, Semenov *et al* 2015). The prolonged open water conditions in the marginal Arctic seas open new prospects for navigation along the Northern Sea Route (NSR) (e.g. Mokhov *et al* 2007, 2016, Khon *et al* 2010, Rogers *et al* 2013, Stephenson *et al* 2013, Larsen *et al* 2014, Barnhart *et al* 2015, Shalina 2015, Aksenov *et al* 2016, Laliberté *et al* 2016). The NSR shortens the transport distance from northern Europe to northeast Asia and northwest North America by up to 50% relative to the southern routes through Suez or Panama Canal. Therefore, ongoing Arctic sea ice decline promotes the NSR as a potential alternative for intercontinental navigation between Atlantic and Pacific regions in forthcoming decades. One of the first estimates of projected perspectives for the NSR (e.g. Khon *et al* 2010) was based on simulations from the Coupled Model Intercomparison Project Phase 3 (Meehl *et al* 2007).

Along with new perspectives, sea ice retreat in the Arctic can however cause new problems. Although, the Arctic marine navigation and other offshore and shelf activities become possible, risks due to waves and associated storm surges and coastal erosion are likely to increase (Overeem *et al* 2011, Dobrynin *et al* 2012, Khon *et al* 2013, 2014). Simulations of wind-wave activity in the Arctic (Khon *et al* 2014) with the wave model in combination with a regional climate model demonstrate overall growth in wave height in the Arctic in the 21st century. Model results also predict more frequent occurrence of extreme winds and waves in different areas of the Arctic Ocean, in particular along the NSR. This is due to both regional wind intensification and longer wave fetches caused by ice retreat.

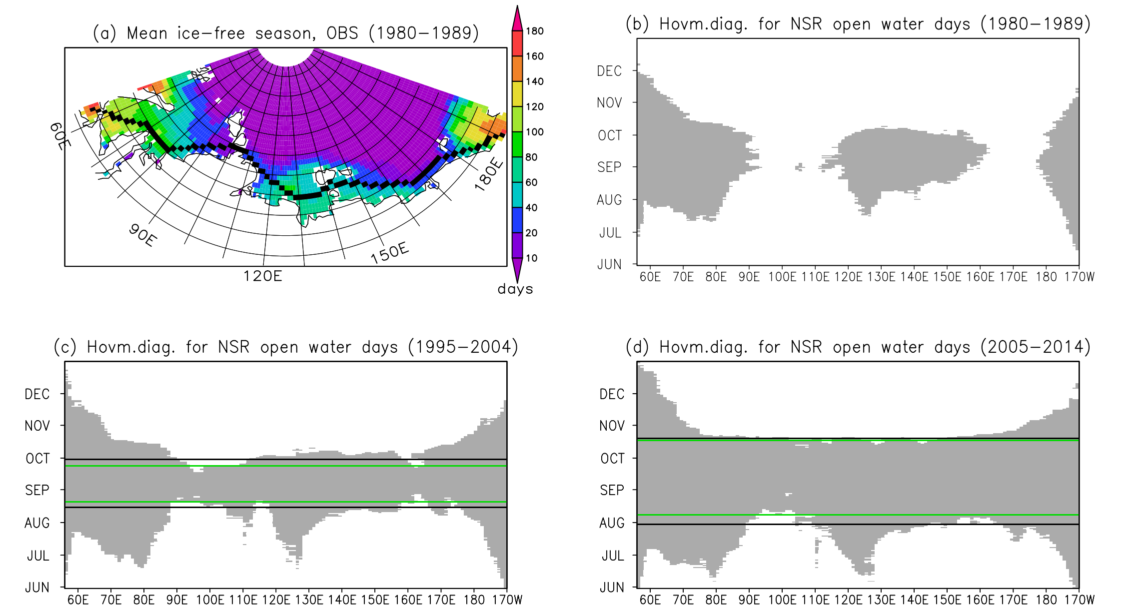

Figure 1. (*a*) The optimal transit route of the NSR (Mulherin *et al* 1999) from Kara to Bering Straits used in this study and climatological mean ice-free season (days) for 1980–1989 from satellite data (Peng *et al* 2013). (*b*)–(*d*) Hovmueller diagrams showing seasonal formation of open water (gray shading) along the NSR as a function of the NSR longitude for three decades 1980–1989 (*b*), 1995–2004 (*c*) and 2005–2014 (*d*) according to the satellite data. Horizontal black (green) lines show the first and last day of 80% (90%) ice-free NSR (see text for details).

In this paper we focus on the transit time window of the NSR allowing intercontinental marine navigation between Atlantic and Pacific regions. For this purpose we introduce a novel approach to calculate the first (start) and the last (end) dates of the NSR transit navigation and the duration of transit navigation. The estimates are based on projections from the Coupled Model Intercomparison Project Phase 5 (CMIP5) (Taylor *et al* 2012).

Most recently, Melia *et al* (2016) estimated navigation season length along the NSR with a variety of possible trans-Arctic routes including trans-polar directions. We note that due to severe Arctic climate and higher safety standards required, near coast routes will be the only realistic solutions for the coming decades. Therefore we focus on the recommended optimal routes for transit navigation along the Russian Arctic coast (Mulherin *et al* 1999). Furthermore, due to the large CMIP5 model spread in simulating Arctic sea ice concentration particularly on the regional scale (Semenov *et al* 2015), we select analysis for only those models that are able to realistically simulate present day length of the NSR navigation season and its variability. In contrast to other studies based on the CMIP5 multimodel means our estimates are based on the most realistic models that were selected using objective criteria.

2. Data and methods

Simulations with global climate models participating within the CMIP5 were used to estimate possible changes in the NSR transit navigation season for the 21st century. The simulations are driven by combined historical-Representative Concentration Pathway 4.5 (RCP4.5) and 8.5 (RCP8.5) scenarios (Van Vuuren *et al* 2011). We analyze data of 25 models that provide daily sea ice concentration (SIC) as output variable.

The daily SIC data (Peng *et al* 2013) are derived from the Nimbus-7 Scanning Multichannel Microwave Radiometer (SMMR) and the Defense Meteorological Satellite Program (DMSP) passive microwave radiometers: Special Sensor Microwave Imager (SSM/I) and Special Sensor Microwave Imager/Sounder (SSMIS) using the NASA team algorithm.

For a particular day, any grid cell with SIC less then 15% is considered as ice-free (or open water). This criterion is broadly used as a threshold for the possible navigation of light ice-class ships. Different criteria, such as 25% and 50% sea-ice concentration requiring ice-strengthened vessels for safe navigation are also studied (e.g. Mokhov *et al* 2016).

Although the choice of optimal route is dependent on current meteorological conditions, several optimal NSR lines can be established based on long-term environmental observations. One of the recommended optimal routes (Mulherin *et al* 1999) for the transit navigation was digitalized onto the 1×0.5 longitude-latitude grid (figure 1(*a*)). The 1×0.5 grid maintains the width and length of cells along the NSR approximately equal ($\backsim 55 \times 55$ km at 60 N). Both satellite and model sea ice concentrations were interpolated onto the same 1×0.5 longitude-latitude grid.

3. Results

In the present paper we develop a new method to calculate characteristics (such as start, end dates and duration) of transit navigation between Atlantic and

Table 1. Mean $T_{80\%}$, $T_{90\%}$ (2005–2014) and their trends $T'_{80\%}$, $T'_{90\%}$ (1980–2014) for the NSR transit window as observed and simulated by five selected models under combined historical-RCP4.5 scenario. $T_{80\%}$ ($T_{90\%}$) is computed as the number of days per year with a length of ice-free passage exceeding 80% (90%) of the NSR extent from Kara to Bering Straits. Standard deviations are given in brackets.

Data	Satellite	CNRM-CM5	HadGEM2-CC	MIROC-ESM-CHEM	MPI-ESM-LR	MPI-ESM-MR	Model mean
$T_{80\%}$, days	73 (±11)	64 (±21)	80 (±18)	60 (±43)	84 (±34)	66 (±32)	71 (±30)
$T'_{80\%}$, day/year	2.4 (±0.4)	2.5 (±0.3)	2.3 (±0.4)	2.3 (±0.5)	2.9 (±0.5)	1.9 (±0.6)	2.4 (±0.4)
$T_{90\%}$, days	62 (±13)	44 (±28)	57 (±25)	47 (±43)	65 (±34)	40 (±37)	51 (±33)
$T'_{90\%}$, day/year	2.1 (±0.3)	1.8 (±0.3)	2.0 (±0.4)	1.9 (±0.5)	2.5 (±0.5)	1.3 (±0.5)	1.9 (±0.4)

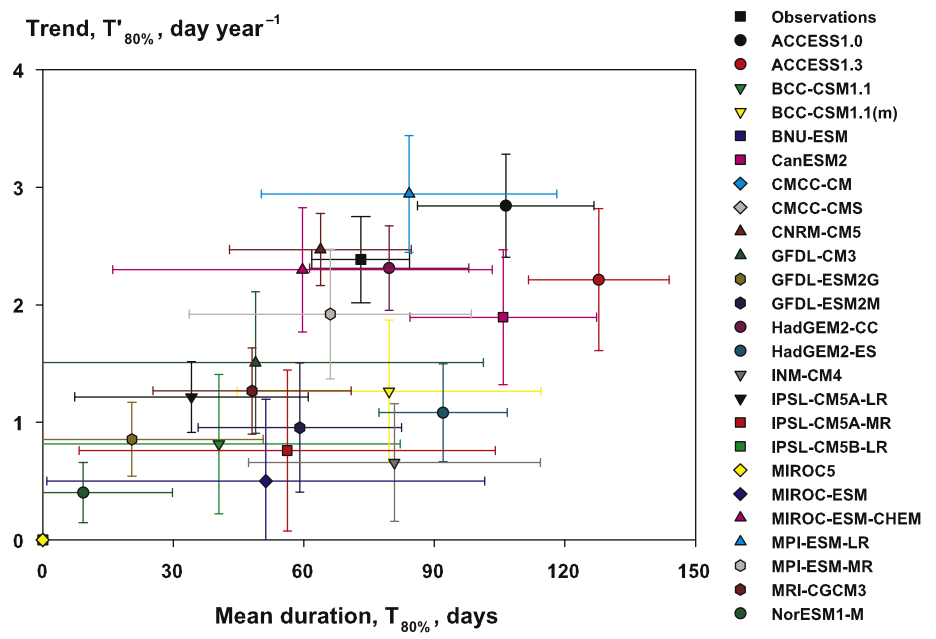

Figure 2. Validation of the present-day transit navigation throughout the NSR from Kara to Bering Straits: climatological mean duration $T_{80\%}$ (number of days with ice-free passage exceeding 80% of the NSR extent) for 2005–2014 and its trend $T'_{80\%}$ over 1980–2014 for satellite data (Peng *et al* 2013) and CMIP5 ensemble.

Pacific regions along the NSR. We assign a particular day as a potentially navigable one for the transit navigation when the daily length of ice-free passage exceeds a threshold of 80% of the total NSR extent. The choice of the threshold is based on the assumption that navigation through the 80% ice-free passage can be easily realized with a minor icebreaker support. A stronger criterion with the ice-free passage exceeding 90% of the NSR is also used in this study. Our approach requires nearly open passage for a particular day and, therefore, can be applied for uninterrupted voyages through the whole NSR. All calculations were made for one of the optimal transit routes (Mulherin *et al* 1999) shown in figure 1(*a*).

The Hovmueller diagrams (figures 1(*b*)–(*d*)) demonstrate intra-annual evolution of open water season along the NSR as a function of longitude, where regional start and end dates of open water season can be observed. Observations indicate that the transit 'end-to-end' navigation throughout the whole NSR has become possible only over the last two decades (figures 1(*c*) and (*d*)). In contrast, over the period 1980–1989 the transit navigation was not possible without ice-breaker support (figure 1(*b*)). Also, the duration of the transit navigation has been growing within the last two decades (figures 1(*c*) and (*d*)). To quantify the duration of the NSR transit navigation we calculated the first and last days when the daily length of ice-free passage exceeds a threshold of 80% and 90% of the total NSR extent (shown by black and green horizontal lines in figures 1(*c*) and (*d*), respectively). The 90% threshold for ice-free passage shortens marine navigation along the NSR by ∽10 days according to sattelite data and by ∽20 days according to multi-model estimate (table 1) for the period 2005–2014.

Figure 2 represents a validation of the CMIP5 models' results against satellite data in terms of their ability to reproduce means ($T_{80\%}$) and trends ($T'_{80\%}$) of the NSR transit time window for the present-day climate. The error bars in figure 2 represent corresponding standard deviations for observations and model simulations. The method of models' evaluation is similar to that performed in Khon *et al* (2010) except for the error bars that were also added to model simulations results for a better comparison. The CMIP5 model ensemble demonstrates a broad spread of model estimates with a tendency to underestimate

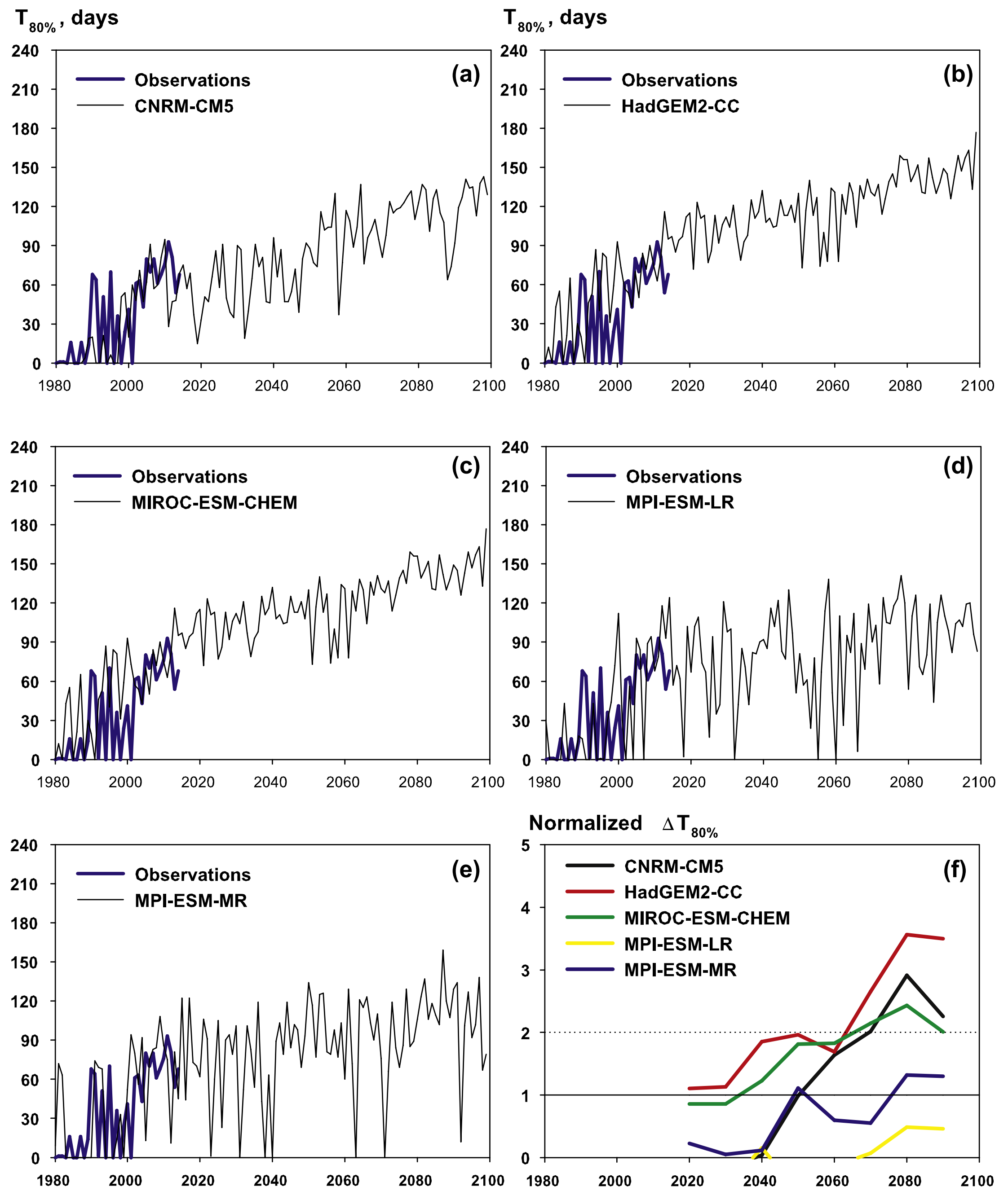

Figure 3. Time-series of the NSR transit duration ($T_{80\%}$) as observed and simulated by selected models under the moderate greenhouse gas concentration scenario RCP 4.5: CNRM-CM5 (*a*), HadGEM2-CC (*b*), MIROC-ESM-CHEM (*c*), MPI-ESM-LR (*d*), MPI-ESM-MR (*e*). (*f*) Consecutive 10-year mean changes (relative to 2005–2014) of the NSR transit duration ($T_{80\%}$) normalized by model standard deviations for period 2005–2014.

satellite data in the majority of models. We assume that a particular model is able to reproduce the present-day NSR transit duration if its error bars intersect observational intervals of variability. Five models (CNRM-CM5, HadGEM2-CC, MIROC-ESM-CHEM, MPI-ESM-LR, MPI-ESM-MR) were found to be sufficient for reproducing both mean values and trends of the observed NSR transit navigation and, therefore, were selected for the further analysis. According to satellite observations mean $T_{80\%}$ ($T_{90\%}$) amounts to about 73 (62) days for 2005–2014 period and its trend $T'_{80\%}$ ($T'_{90\%}$) over 1980–2014 period is estimated to be about 24 (21) days per decade (table 1). In general, modern climate models are able to reproduce means ($T_{80\%}$, $T_{90\%}$) and trends ($T'_{80\%}$, $T'_{90\%}$) of the NSR transit time window over the last few decades (table 1). However, a spread of year-to-year variability is much larger for model simulations compared to satellite data (figure 2; table 1).

Individual time-series of the NSR transit duration for the selected models are shown in figures 3(*a*)–(*e*) together with the satellite data. As can be seen in figures 3(*a*)–(*e*) the selected models show a relatively realistic representation of the NSR transit navigation time over the last decades as also shown in figure 2. The models' long-term tendency of increasing $T_{80\%}$ is accompanied with stronger interannual and multidecadal variability in the 21st century.

Table 2. Projected mean $T_{80\%}$ of the NSR transit window calculated for five selected models and three different decades using two greenhouse gas concentration scenarios RCP4.5 and 8.5. $T_{80\%}$ is computed as the number of days per year with a length of ice-free passage exceeding 80% of the NSR extent from Kara to Bering Straits. Standard deviations are given in brackets.

$T_{80\%}$, days	CNRM-CM5	HadGEM2-CC	MIROC-ESM-CHEM	MPI-ESM-LR	MPI-ESM-MR	Model mean
2016–2025						
RCP4.5	52 (±20)	100 (±18)	97 (±39)	67 (±35)	73 (±35)	78 (±29)
RCP8.5	55 (±27)	100 (±19)	95 (±38)	78 (±35)	55 (±32)	77 (±30)
2046–2055						
RCP4.5	84 (±22)	116 (±18)	139 (±21)	66 (±37)	102 (±23)	101 (±24)
RCP8.5	100 (±12)	137 (±13)	155 (±15)	108 (±36)	89 (±37)	118 (±23)
2090–2099						
RCP4.5	127 (±16)	150 (±15)	148 (±12)	102 (±13)	98 (±39)	125 (±19)
RCP8.5	174 (±11)	200 (±11)	252 (±16)	164 (±12)	169 (±24)	192 (±15)

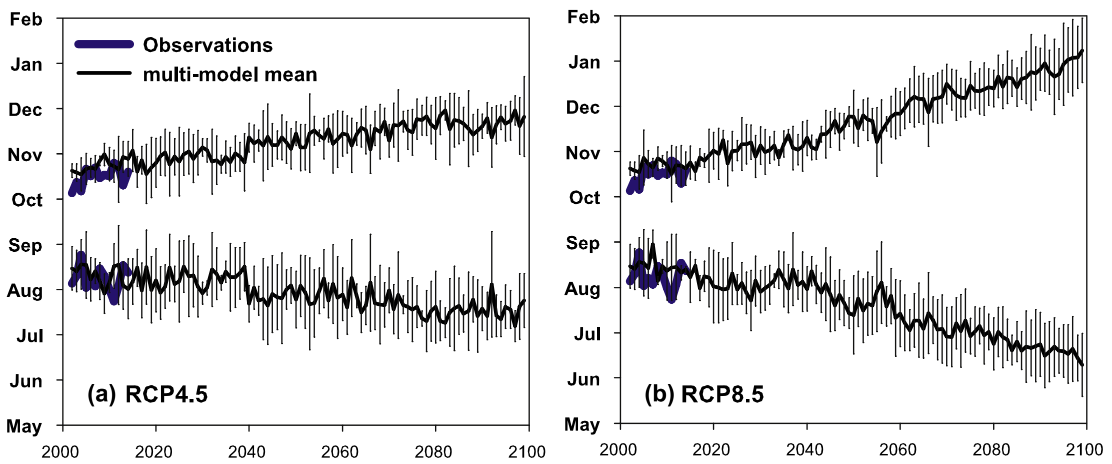

Figure 4. Ensemble-mean projections of the beginning and the end of the NSR transit navigation period ($T_{80\%}$) according to scenario RCP 4.5 (*a*) and 8.5 (*b*) averaged by using five selected models (CNRM-CM5, HadGEM2-CC, MIROC-ESM-CHEM, MPI-ESM-LR, MPI-ESM-MR). Satellite data is shown by the blue line. Vertical bars represent corresponding standard deviations based on estimates of the selected models.

Estimated long-term trends also vary broadly within the five selected models shown by consecutive 10-year mean changes (relative to 2005–2014) of the NSR duration normalized by their standard deviations σ for the 2005–2014 period (figure 3(*f*)). Two models (MPI-ESM-LR, MPI-ESM-MR) demonstrate slow or moderate growth (being less or just slightly exceeding 1 σ) and three other models project stronger growth (more than 2–3 σ) by the end of the 21st century (figure 3(*f*)). The quantitative estimates for the projected $T_{80\%}$ ($T_{90\%}$) are given in table 2 (table S1 available at stacks.iop.org/ERL/12/024010/mmedia) for different decades in the 21st century. For the next few decades three models (CNRM-CM5, MPI-ESM-LR, MPI-ESM-MR) demonstrate a slow down in the growth rate of the NSR navigation season length (figure 3(*f*)) and even its decrease in the next decade (CNRM-CM5, MPI-ESM-LR; table 2, table S1). In general, multi-model mean estimates show an increase of mean $T_{80\%}$ ($T_{90\%}$) to ∽4 (3.5) months at the end of 21st century according to RCP4.5 and to ∽6.5 (6) months according to RCP8.5 (table 2, table S1).

Figure 4 presents projected time-series for the start and end dates of the NSR transit navigation as observed and simulated by ensemble-mean amongst selected models using scenarios RCP 4.5 (*a*) and 8.5 (*b*). As can be seen from figure 4, the observed start and end dates are sufficiently well reproduced by selected models with observational estimates varying within the interval of a model standard deviation. According to the RCP4.5 scenario, anticipated increase in $T_{80\%}$ is a result of comparable contributions from the later end and earlier start by the end of the 21st century. The simulated navigation start (end) date for the NSR is estimated to occur in the mid-July (mid-November) according to RCP4.5 and in the mid-June (end of December) according to RCP8.5 by the end of 21st century (figure 4, table S2).

The NSR transit is strongly affected by the accessibility of the region around Severnaya Zemlya (90°E–120°E) where the number of ice-free days has a well pronounced local minimum (figure 1). More severe ice conditions and, therefore, shorter local navigation time within this sector strongly restricts the transit time through the entire NSR in present climate conditions (figure S1) as shown by observations and models (CNRM-CM5, HadGEM2-CC, MIROC-ESM-CHEM). By the end of the 21st century, however, the difference between the local (90 °E–120 °E) and the entire NSR navigation $T_{80\%}$ decreases implying an insignificant role of local minima on the entire NSR navigation according to model results in the future (figure S1).

4. Summary and conclusions

We note that along with the model and scenario related uncertainties the estimates of future prediction are impacted by internal variability that may result, in particular, in prediction uncertainty of about two decades for the timing of the summer ice-free Arctic (Jahn *et al* 2016). Arctic climate changes are characterized by a strong multi-decadal variability that may also widen the uncertainty range (Polyakov *et al* 2003, Polyakov *et al* 2013). Furthermore, the result can be very sensitive to a method of weighting of models' results as was shown by applying a Bayesian approach to the Arctic sea ice area projections (Eliseev and Semenov 2016).

In conclusion, we present new estimates for the NSR transit window allowing intercontinental navigation in the 21st century based on satellite data and CMIP5 ensemble of climate models. A novel approach is introduced to calculate start, end dates and duration of navigation season along the NSR. The novelty of the approach used in this study consists of a new way of calculation of the accessibility of the NSR based on daily data. We consider the NSR as a potentially navigable one (with a minor icebreaker support) when the daily ice-free passage exceeds a particular threshold. In contrast to a previous method (Khon *et al* 2010) we calculate accessibility along the whole route for each day (using a given threshold, e.g. 80%). This method is more accurate and provides us with the first and last days of the navigation season.

We selected only those climate models that are able to reproduce both mean values and trends of the observed NSR transit navigation over the last few decades. According to the selected models, the observed growth rate of the NSR navigation will slow down over the next few decades with RCP4.5 scenario. By the end of this century the NSR transit navigation period $T_{80\%}$ ($T_{90\%}$) is estimated to be about 4 (3.5) and 6.5 (6) months according to RCP4.5 and 8.5, respectively, based on the ensemble-mean estimates. We note that projected trends for the end date of the navigation season are found to be stronger compared to the trends for the start date.

Acknowledgments

This work was supported by the Russian Science Foundation (project no. 14-17-00647) with additional support from the Programs of the Russian Academy of Sciences and Russian Foundation for Basic Research (Grant 14-05-00639).

References

Aksenov Y, Popova E E, Yool A, Nurser A J G, Williams T D, Bertino L and Bergh J 2016 On the future navigability of Arctic sea routes: high-resolution projections of the Arctic Ocean and sea ice *Mar. Policy* **75** 300–17

Barnhart K R, Miller C R, Overeem I and Kay J E 2015 Mapping the future expansion of Arctic open water *Nat. Clim. Change* **6** 280–5

Dobrynin M, Murawsky J and Yang S 2012 Evolution of the global wind wave climate in CMIP5 experiments *Geophys. Res. Lett.* **39** L18606

Eliseev A V and Semenov V A 2016 Climate changes in the Arctic during the 21st century: model ensemble estimates model accounting for realism in the present-day climate simulation *Dokl. Earth Sci.* **471** 1183–7

Jahn A, Kay J E, Holland M M and Hall D M 2016 How predictable is the timing of a summer ice-free Arctic? *Geophys. Res. Lett.* **43** 9113–20

Khon V C, Mokhov I I and Pogarskii F A 2013 Estimating changes of wind-wave activity in the Arctic Ocean in the 21st century using the regional climate model *Dokl. Earth Sci.* **452** 1027–9

Khon V C, Mokhov I I, Pogarskiy F A, Babanin A, Dethloff K, Rinke A and Matthes H 2014 Wave heights in the 21st century Arctic Ocean simulated with a regional climate model *Geophys. Res. Lett.* **41** 2956–61

Khon V C, Mokhov I I, Latif M, Semenov V A and Park W 2010 Perspectives of Northern Sea Route and Northwest Passage in the twenty-first century *Clim. Change* **100** 757–68

Laliberté F, Howell S E L and Kushner P J 2016 Regional variability of a projected sea ice-free Arctic during the summer months *Geophys. Res. Lett.* **43** 256–63

Larsen J N, Anisimov O A, Constable A, Hollowed A B, Maynard N, Prestrud P, Prowse T D and Stone J M R 2014 Polar regions *Climate Change 2014: Impacts, Adaptation, and Vulnerability. Part B: Regional Aspects. Contribution of Working Group II to the Fifth Assessment Report of the Intergovernmental Panel on Climate Change* ed V R Barros *et al* (Cambridge: Cambridge University Press) pp 1567–612

Meehl G A *et al* 2007 The WCRP CMIP3 multimodel dataset—A new era in climate change research *Bull. Am. Meteorol. Soc.* **88** 1383–94

Melia N, Haines K and Hawkins E 2016 Sea ice decline and 21st century trans-Arctic shipping routes *Geophys. Res. Lett.* **43** 9720–8

Mokhov I I, Khon V C and Roeckner E 2007 Variations in the ice cover of the Arctic Basin in the 21st century based on model simulations: estimates of the perspectives of the Northern Sea Route *Dokl. Earth Sci.* **415** 759–63

Mokhov I I, Khon V C and Prokof'eva M A 2016 New model estimates of changes in the duration of the navigation period for the Northern Sea Route in the 21st century *Dokl. Earth Sci.* **468** 641–5

Mulherin N D, Eppler D T and Sodhi D S 1999 NSRSIM2A: a time and cost prediction model for Northern Sea Route Shipping *INSROP Working Paper 150* p 142

Overeem I *et al* 2011 Sea ice loss enhances wave action at the Arctic coast *Geophys. Res. Lett.* **38** L17503

Peng G, Meier W N, Scott D J and Savoie M H 2013 A long-term and reproducible passive microwave sea ice concentration data record for climate studies and monitoring *Earth Syst. Sci. Data* **5** 311–8

Polyakov I V *et al* 2003 Long-term ice variability in Arctic marginal seas *J. Clim.* **16** 2078–85

Polyakov I V *et al* 2013 Recent oceanic changes in the Arctic in the context of long-term observations *Ecol. Appl.* **23** 1745–64

Rogers T S, Walsh J E, Rupp T S, Brigham L W and Sfraga M 2013 Future Arctic marine access: analysis and evaluation of observations, models, and projections of sea ice *Cryosphere* **7** 321–32

Semenov V A, Martin T, Behrens L K and Latif M 2015 Arctic sea ice area in CMIP3 and CMIP5 climate model ensembles—variability and change *The Cryosphere Discuss.* **9** 1077–131

Shalina E V 2015 Ice retreat in the Russian Arctic Seas and assessment of the availability of the Northern Sea Route from satellite passive microwave observations *Izv. Atmos. Oceanic Phys.* **51** 903–13

Stephenson S R, Smith L C, Brigham L W and Agnew J A 2013 Projected 21st-century changes to Arctic marine access *Clim. Change* **118** 885–99

Stroeve J C, Kattsov V, Barrett A, Serreze M, Pavlova T, Holland M and Meier W N 2012 Trends in Arctic sea ice extent from CMIP5, CMIP3 and observations *Geophys. Res. Lett.* **39** L16502

Taylor K E, Stouffer R J and Meehl G A 2012 An overview of CMIP5 and the experiment design *Bull. Am. Meteorol. Soc.* **93** 485–98

Van Vuuren D P, Edmonds J, Kainuma M, Riahi K, Thomson A, Hibbard K, Hurtt G C, Kram T, Krey V and Lamarque J-F 2011 The representative concentration pathways: an overview *Clim. Change* **109** 5–31